

Inverse Bloch Oscillator: Strong Terahertz-Photocurrent Resonances at the Bloch Frequency

K. Unterrainer,* B. J. Keay, M. C. Wanke, and S. J. Allen

Center for Free-Electron Laser Studies, University of California, Santa Barbara, California 93106

D. Leonard, G. Medeiros-Ribeiro, U. Bhattacharya, and M. J. W. Rodwell

Materials and ECE Department, University of California, Santa Barbara, California 93106

(Received 24 October 1995)

We have observed the *inverse Bloch oscillator effect*: resonant changes in the current-voltage characteristics of miniband semiconductor superlattices when the Bloch frequency is resonant with a terahertz field and its harmonics. The resonances consist of a peak in the current accompanied by a decrease of the current at the low bias side. At the highest intensities we observe up to a four-photon resonance. This is an analog of Shapiro steps in a *S-I-S* junction caused by the ac Josephson effect. The increase of the current is caused by stimulated emission of photons and we can estimate the THz gain of the superlattice from the induced current at the resonance.

PACS numbers: 73.50.Fq, 72.20.Ht, 73.20.Dx

In a pioneering paper, Esaki and Tsu proposed high frequency oscillators by tailoring the nonlinear electronic transport properties of semiconductors by fabricating superlattice structures [1]. Minibands are formed, and electrons accelerated by a moderate, constant electric field, E , can perform a repetitive motion of acceleration and Bragg reflection called Bloch oscillation, characterized by the Bloch frequency $\omega_B = eEd/\hbar$, where d is the superlattice period. Bloch oscillation is a well defined normal mode of the system at THz frequencies, where $\omega_B\tau > 1$ [2,3]. However, it took more than two decades before the first observation of Bloch oscillations was made in a degenerate four wave mixing experiment [4] and in a transient THz emission experiment of optical excited electrons [5]. The emission was attributed to quantum beats of wave packets excited in different levels of a Wannier-Stark ladder—the quantum mechanical equivalent for the Bloch oscillator. The observation of continuous Bloch emission from electrically injected carriers in a superlattice has escaped observation so far.

The formation of Bloch oscillations in a dc biased superlattice also influences the dc conductivity. At low bias when the Bloch frequency is not high enough to overcome scattering ($\omega_B\tau < 1$) the electrons never reach the inflection point, and the current in the superlattice direction is given by the Drude conductivity. When the bias is high enough to make Bloch oscillation possible, the electrons start to oscillate in space and stop to contribute to the dc current which leads to negative differential conductivity [6,7].

In this paper we have combined transport and THz spectroscopy to show that dc current driven Bloch oscillation couples to external radiation by either emission or absorption of THz photons. We explore this phenomenon by investigating the *inverse Bloch oscillator effect* which senses changes in the dc conductivity under the influence of an external THz field.

An electron in a superlattice with a dispersion relation

$$\epsilon(k) = E_1 + \Delta/2[1 - \cos(kd)] \quad (1)$$

driven by an electric field $E(t) = E^{\text{dc}} + E^{\text{ac}} \cos(\omega t)$ can be treated in analogy to superconducting ac Josephson junctions [8,9], where the current is given by

$$I = I_c \sin(\Phi) \quad \text{and} \quad \dot{\Phi} = 2 eV/\hbar. \quad (2)$$

The velocity of an electron in a superlattice miniband is given by

$$v(k) = \frac{\Delta d}{2\hbar} \sin(kd) \quad \text{and} \quad \dot{k}d = \frac{e}{\hbar} E(t)d. \quad (3)$$

The solution for the Josephson junction gives the well known Shapiro steps at $V^{\text{dc}} = N\hbar\omega/2e$. This simple analogy predicts Shapiro steps in the dc current of a semiconductor superlattice driven by an ac field at resonances $E^{\text{dc}}d = N\hbar\omega/e$. This indicates that the high frequency field couples to Bloch oscillations. However, Ferreira and Bastard [10] predict that the absorption spectrum of a superlattice should not show any resonances at the Bloch frequency based on the fact that the populations in adjacent Wannier-Stark levels are equal, and emission and absorption should cancel each other. Ferreira and Bastard do not include dissipation which is a critical element in the treatment.

Dissipation can be included in the quasiclassical Bloch oscillator model by solving the Boltzmann equation [11]. For a constant scattering time τ and a photon energy $\hbar\omega$, smaller than the miniband width Δ , the dc current can be written as

$$j = j_0 \sum_{m=0}^{+\infty} J_m^2(eE^{\text{ac}}d/\hbar\omega) \times \left[\frac{(\omega_B + m\omega)\tau}{1 + (\omega_B + m\omega)^2\tau^2} + \frac{(\omega_B - m\omega)\tau}{1 + (\omega_B - m\omega)^2\tau^2} \right], \quad (4)$$

where the J_m are Bessel functions. The dc current is plotted for $eE^{ac}d/\hbar\omega = 0$ (dotted curve in Fig. 1) and for $eE^{ac}d/\hbar\omega = 1.3$ (solid curve in Fig. 1) for $\tau = 1$ ps and $\nu = 0.6$ THz. The curve for $eE^{ac}d/\hbar\omega = 1.3$ shows a strong modulation of the current when the Bloch frequency ω_B equals the applied frequency ω or its higher harmonics.

The THz current at 0.6 THz is also shown in Fig. 1 (dashed curve). Negative conductivity or gain is predicted when the Bloch frequency is $\omega_B > \omega$ and absorption when $\omega_B < \omega$ [11]. Figure 1 demonstrates that the features in the dc current can be correlated with the occurrence of gain or loss. An increased photocurrent implies gain, and a suppression of the current below the dc level corresponds to absorption. In the Wannier-Stark level picture an increased current is caused by stimulated emission of photons through intra Wannier-Stark level transitions, and a suppression is caused by absorption. In a single superlattice miniband this is an unambiguous method of interpreting the induced current since no transport channels through higher subbands exist where a positive induced current can be caused by absorption and subsequent inelastic scattering.

For $\omega_B \rightarrow 0$ the low voltage conductance is proportional to $J_0^2(eE^{ac}d/\hbar\omega)$. At the zeros of J_0 the dc current is expected to be completely quenched by the ac field. This ac localization was also predicted by fully quantum mechanical calculations of the energy levels of a superlattice in an intense periodic electric field [12].

The samples used in this study of the *inverse Bloch oscillator effect* are GaAs/Al_xGa_{1-x}As ($x = 0.3$) superlattices grown on a semi-insulating GaAs substrate by molecular beam epitaxy. The superlattice structure consists of 40 periods of 80 Å wide GaAs wells and 20 Å thick AlGaAs barriers. The superlattice is homogeneously Si doped with a concentration of $n = 3 \times 10^{15}$ cm⁻³. Lightly doped 80 Å thick GaAs setback layers separate the superlattice from 3000 Å thick

GaAs layers ($n = 2 \times 10^{18}$ cm⁻³) which serve as contact regions.

The wave functions of the GaAs wells overlap strongly, and minibands are formed. A band-structure calculation in the envelope function approximation [13] results in a width for the lowest miniband $\Delta = 22$ meV. This means that electrons moving in the lowest miniband are not scattered by optical photons. The effective mass of electrons at the bottom of the miniband is $m^{SL} = 0.07m_0$. The second miniband is separated from the first one by about 100 meV. Thus, for low applied bias (<200 mV), we do not have to consider tunneling to the second miniband.

Superlattice mesas with an area of 8 μm² are formed by dry etching and an ion (H⁺) implantation-isolation process. Ohmic Au/Ge/Ni contacts are fabricated on the top and the bottom of the mesas. A coplanar broad band bow-tie antenna was used to couple the THz electric field to the mesa parallel to the growth direction [14] and enhances the electric field by a factor of 50 to 100. The experiments were performed at 10 K in a temperature controlled flow cryostat with Z-cut quartz windows. The conductance of the superlattice was measured during the microsecond long pulses of THz radiation provided by the UCSB free electron lasers.

The current-voltage characteristics of our superlattice device without THz radiation (dc-IV) can be seen in Fig. 2(a) (curve labeled $I = 0$). The negative dc (NDC) region starts at a bias of 20 mV which corresponds to a critical electric field of 500 V/cm. Assuming that the onset of the NDC region is due to Esaki-Tsu-type localization, we find a scattering time $\tau = 1.3$ ps. The maximum current density is about 100 A/cm². The IV curve shows a small asymmetry: For positive bias (injection from the top contact) we find a more pronounced NDC than for negative bias. This asymmetry is present in all devices and we think is due to the different geometry of top and bottom contacts or due to inhomogeneity in the doping.

The influence of an external THz electric field on the superlattice current is shown in Fig. 2(a) for a free electron laser (FEL) frequency of 0.6 THz. The dc current is measured during the FEL pulse as the voltage bias is changed. The curves in Fig. 2(a) are shown for increasing ac field strength (the curves are displaced downward with increasing intensity for clarity). At low intensities an additional peak emerges in the NDC region. We attribute the first additional peak to a resonance of the external laser field with Bloch oscillation, $\omega_B = \omega$. When the intensity is increased further the first peak starts to decrease, and a second peak at about twice the voltage of the first peak is observed and assigned to a two-photon resonance. At the highest intensities we observe a four-photon resonance. The initial current peak of the dc-IV decreases with increasing intensity indicating the onset of ac localization [15]. At very high intensities a small bump at the original position of the peak recovers.

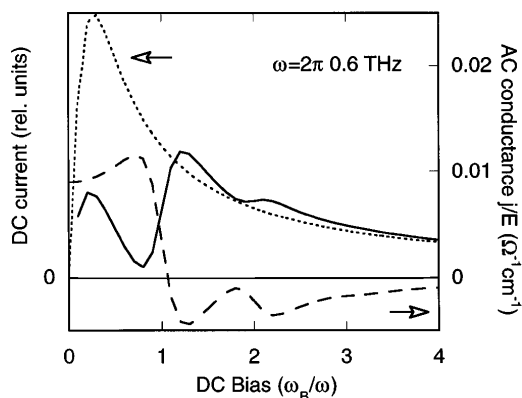


FIG. 1. Calculation of the superlattice current as a function of the applied bias for $eE^{ac}d/\hbar\omega = 0$ (dotted curve) and for $eE^{ac}d/\hbar\omega = 1.3$ (solid curve). The absorption coefficient (dashed curve) is shown for $eE^{ac}d/\hbar\omega = 1.3$. THz gain is predicted when the induced dc current shows an increase.

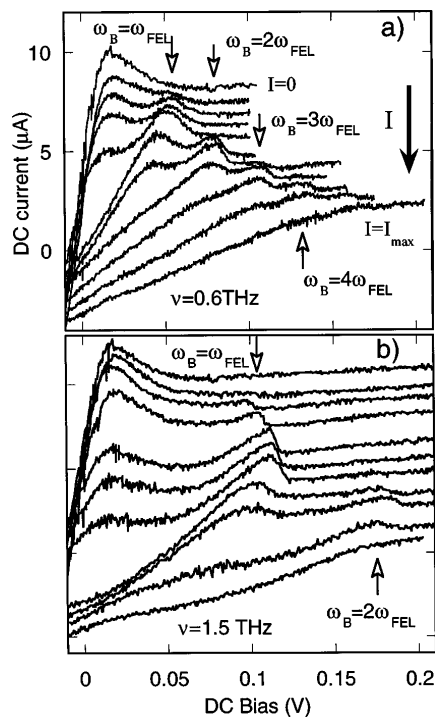


FIG. 2. dc current-voltage curve for increasing FEL intensity (the curves are shifted downwards for increasing laser intensity). The FEL frequency was fixed to 0.6 THz (a) and to 1.5 THz (b). In the NDC region additional features occur attributed to resonances at the Bloch frequency and its subharmonics.

In Fig. 2(b) the results for a laser frequency of 1.5 THz are shown. The peaks are shifted to higher voltages and are much more pronounced. Only the fundamental and the second harmonic is observed, since, for a given E^{ac} , $eE^{ac}d/\hbar\omega$ is smaller at higher frequencies. In addition, we observe a suppression of the current value in between the peaks. The peaks show a clear asymmetry with a steeper slope on the high voltage side. This asymmetry is different from the shape of the peak of original dc-IV which shows a steeper slope at the low voltage side.

In Fig. 3 the peak positions are shown as a function of FEL frequency. The relationship is linear, and the slopes of the N th harmonic are N times the slope of the one-photon resonance. The magnitude of the slope is larger than expected from a voltage drop across the whole superlattice. The most reasonable explanation is that a high electric field domain is formed which extends over approximately one-third of the superlattice [16]. For this stable situation the electric field in the low field domain is below the critical field for localization and puts this part of the superlattice in the high conductive miniband transport regime.

The formation of a high field domain could also explain the discrepancies between the values for the scattering times deduced from the dc-IV and from the THz measurements. If the onset of the NDC is more likely caused by domain formation, localization over a

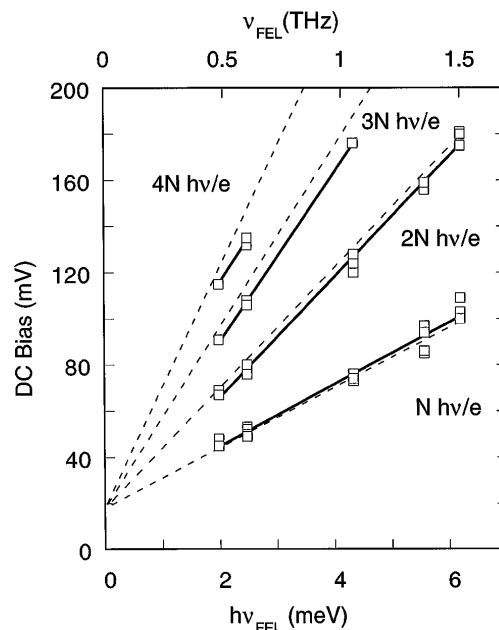


FIG. 3. dc bias positions of the induced current peaks versus FEL frequency.

fraction of the superlattice, and not by the onset of localization over the entire superlattice, the value for the scattering time which we derived from the assumption of uniform localization is incorrect. Indeed, we observe resonances with Bloch oscillation only for frequencies higher than 480 GHz which corresponds to a scattering time of 0.35 ps, approximately 3–4 times shorter than the previous estimate. This value is consistent with earlier cyclotron resonance measurements (magnetic field perpendicular to the growth direction) which showed in low doped samples also a coherence length of ≈ 10 superlattice periods [17].

In Fig. 4 the intensity dependence of the current at the different resonances at 0.6 THz is shown. In addition, the predicted current from Eq. (4) is plotted. The absolute value of the electric field is obtained from a fit to the maximum of the current of the one-photon resonances. The coincidence of the first maxima for the higher photon resonances is very good. Thus, we can use the fit to the maxima to calibrate our electric field in the sample. A discrepancy exists for the predicted smaller oscillations at higher intensities which do not show up in the experimental data. In addition to the main maximum, a second peak is observed for the one-photon resonance which coincides with a minimum of the calculation. The two-photon resonance shows the same feature which cannot be explained by the simple calculation with a constant scattering time.

A positive photocurrent in the NDC is caused by stimulated emission of photons (electrons move downwards in the Wannier-Stark ladder) [18]. From the value of the photocurrent we can estimate the power transfer for

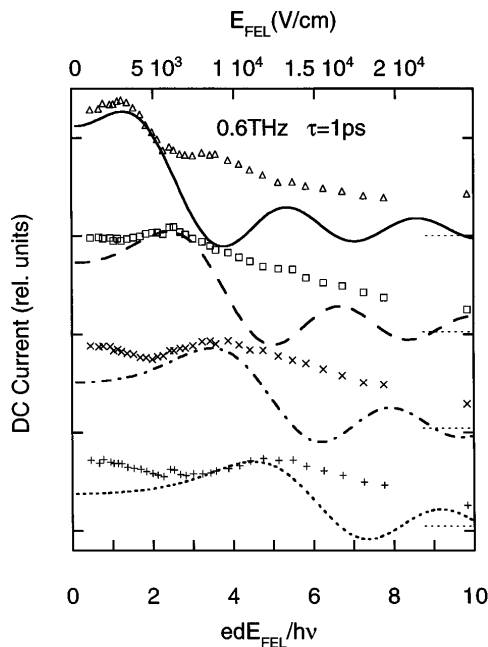


FIG. 4. Data points show the intensity dependence of the current for constant dc bias at different resonance positions at 0.6 THz. The upper curve shows the behavior at a bias of 45 mV, where the one-photon resonance occurs; the other curves show the behavior at the bias positions of the higher resonances. The lines show the predicted current at these resonances as a function of ac field strength.

the dc electric field into the photon field to be about 50 nW (0.56 W/cm^2 in the mesa). The intensity of the ac field inside the superlattice at the maximum of the one-photon resonance is 42 kW/cm^2 which leads to a total THz amplification coefficient of our superlattice mesa of 1.3×10^{-5} . Assuming a 50Ω impedance of the bow-tie structure, we estimate a negative THz conductance of $1.3 \times 10^{-4} (\Omega \text{ cm})^{-1}$ which compares to the theoretical value of $5 \times 10^{-3} (\Omega \text{ cm})^{-1}$. The experiment demonstrates that a superlattice is a possible gain medium for THz oscillators, however, the gain is very small and would hardly overcome resonator losses.

In conclusion, we have observed multiphoton resonances with Bloch oscillation in a superlattice in a dc electric field. Our results show clearly that the external radiation couples to Bloch oscillations, contrary to theoretical suggestions that THz radiation would not couple to a uniform Wannier-Stark ladder. We conclude that this result is intimately related to dissipation and line broadening of the otherwise identical states in the ladder: Absorption appears above the Wannier-Stark splitting ($\omega_B < \omega$) and gain below ($\omega_B > \omega$). The effect is

an analogy to Shapiro steps in S - I - S junctions that support the ac Josephson effect.

The authors would like to thank the staff at the Center for Free-Electron Laser studies: J.R. Allen, D. Enyeart, J.P. Kaminski, G. Ramian, and D. White. Funding for the Center for Free-Electron Laser studies is provided by the Office of Naval Research. This research project was also supported by the Army Research Office, the National Science Foundation, and the Air Force Office of Scientific Research. One of us (K.U.) was supported by a Schrödinger fellowship of the Austrian Science Foundation.

*Present address: Institute for Solid State Electronics, Technical University Vienna, A-1040 Vienna, Austria.

- [1] L. Esaki and R. Tsu, *IBM J. Res. Dev.* **14**, 61 (1970).
- [2] J.B. Krieger and G.F. Iafrate, *Phys. Rev. B* **33**, 5494 (1986).
- [3] A.M. Bouchard and M. Luban, *Phys. Rev. B* **47**, 6815 (1993).
- [4] J. Feldmann *et al.*, *Phys. Rev. B* **46**, 7252 (1992).
- [5] C. Waschke *et al.*, *Phys. Rev. Lett.* **70**, 3319 (1993).
- [6] A. Sibille, J.F. Palmier, H. Wang, and F. Mollot, *Phys. Rev. Lett.* **64**, 52 (1990).
- [7] H. T. Grahn, K. von Klitzing, K. Ploog, and G.H. Döhler, *Phys. Rev. B* **43**, 12094 (1991).
- [8] P.G. de Gennes, *Superconductivity of Metals and Alloys* (W. A. Benjamin Inc., New York, 1966); P.G. de Gennes, "Phénoménologie des Superfluides et Supraconducteurs" (lecture notes).
- [9] A. A. Ignatov, K.F. Renk, and E.P. Dodin, *Phys. Rev. Lett.* **70**, 1996 (1993).
- [10] G. Bastard and R. Ferreira, *C.R. Acad. Sci.* **312**, 971 (1991); R. Ferreira and G. Bastard, *Surface Sci.* **229**, 424 (1990).
- [11] V. V. Pavlovich and E. M. Epshtein, *Sov. Phys. Semicond.* **10**, 1196 (1976); F.G. Bass and E.A. Rubinshtein, *Sov. Phys. Solid State* **19**, 800 (1977).
- [12] M. Holthaus, *Phys. Rev. Lett.* **69**, 351 (1992); J. Zak, *Phys. Rev. Lett.* **71**, 2623 (1993); D.H. Dunlap and V.M. Kenkre, *Phys. Rev. B* **34**, 3625 (1986).
- [13] G. Bastard, *Phys. Rev. B* **24**, 5693 (1981).
- [14] B. J. Keay *et al.*, in *The Physics of Semiconductors: Proceedings of the 22nd International Conference Vancouver, Canada*, edited by D.J. Lockwood (World Scientific, Singapore, 1995), p. 1055.
- [15] A. A. Ignatov *et al.*, *Ann. Phys.* **3**, 137 (1994).
- [16] A. Sibille *et al.*, *Superlattices Microstruct.* **13**, 247 (1993).
- [17] T. Duffield, *Phys. Rev. Lett.* **56**, 2724 (1986).
- [18] P. S. S. Guimaraes *et al.*, *Phys. Rev. Lett.* **70**, 3792 (1993); B. J. Keay *et al.*, *Phys. Rev. Lett.* **75**, 4102 (1995).